CELL TECHNOLOGIES IN BIOLOGY AND MEDICINE

Neural Progenitor and Hemopoietic Stem Cells Inhibit the Growth of Low-Differentiated Glioma

V. P. Baklaushev[1,2], N. F. Grinenko[1], E. A. Savchenko[1], S. N. Bykovskaya[2], G. M. Yusubalieva[1,2], I. V. Viktorov[1] A. S. Bryukhovetskii[3], I. S. Bryukhovetskii[3], and V. P. Chekhonin[1,2]

Translated from *Kletochnye Tekhnologii v Biologii i Meditsine*, No. 4, pp. 183-190, December, 2011
Original article submitted July 15, 2011

The effects of neural progenitor and hemopoietic stem cells on C6 glioma cells were studied in *in vivo* and *in vitro* experiments. Considerable inhibition of proliferation during co-culturing of glioma cells with neural progenitor cells was revealed by quantitative MTT test and bromodeoxyuridine incorporation test. Labeled neural progenitor and hemopoietic stem cells implanted into the focus of experimental cerebral glioma C6 survive in the brain of experimental animals for at least 7 days, migrate with glioma cells, and accumulate in the peritumoral space. Under these conditions, neural progenitor cells differentiate with the formation of long processes. Morphometric analysis of glioma cells showed that implantation of neural progenitor and hemopoietic stem cells is accompanied by considerable inhibition of the growth of experimental glioma C6 in comparison with the control. The mechanisms of tumor-suppressive effects of neural and hemopoietic stem cells require further investigation.

Key Words: *glioma C6; neural progenitor cells; hemopoietic stem cells*

Glioblastoma multiforme, the most invasive low-differentiated tumor, is characterized by extremely poor prognosis due to rapid progressive growth and low efficiency of standard treatment [2]. All current methods, including surgical resection of glioblastoma and radio- and chemotherapy aimed at removal of tumor cells, have little effects on glioma cells that actively invade the nerve tissue. In light of this, of particular importance is the search for new methods aimed at reprogramming of tumor cells by increasing the degree of their differentiation, induction of apoptosis, inactivation of adhesion and migration, *etc*., rather that their removal.

Recent experiments demonstrated that neural stem (NSC) and progenitor cells (NPC) can suppress the growth of glioblastoma multiforme [6]. During ontogent, these cells produce factors regulating not only differentiation and chemotaxis, but also the balance of pro- and antiapoptotic signals, *etc*. *In vivo* studies showed that normal SC and progenitor cells migrating into the tumor and peritumoral zone can transmit differentiation signals to glioblastoma cells thereby reducing their proliferative activity [7]. Molecular mechanisms of this effect are now intensively studied. It is hypothesized that gap junctions and adhesion contacts between NPC and glioma cells and secreted

[1]Department of Fundamental and Applied Neurobiology, V. P. Serbskii State Research Center of Forensic and Social Psychiatry, Mitistry of Health Care and Social Development of the Russian Federation, Moscow; [2]Department of Medical Nanobiotechnologies and Department of Cell Technologies and Regenerative, N. I. Pirogov Russian State Medical University; [3]NeuroVita Clinics of Restorative and Intervention Neurology and Therapy, Moscow, Russia. ***Address for correspondence:*** serpoff@gmail.com. V. P. Baklaushev.

0007-4888/12/1524-0497 © 2012 Springer Science+Business Media, Inc.

signals, *e.g.* BMP7 [3] and IL-18 [13], can play an important role in transmission of inhibitory signal from NPC to tumor cells. Particular attention is given to bone marrow protein family (BMP), because they trigger cell differentiation under normal conditions [4].

According to neurogenesis concept, astroglial progenitor cells are the source of low-differentiated gliomas [5]. The facts that tumor cells originate from abnormal progenitor cells partially explains their sensitivity to signals inhibiting proliferation of phenotypically similar neural and glial progenitor cells [11].

Both NPC and hemopoietic SC (HSC) can migrate to the pathological focus, the site of hyperexpression of CXC- and CC-chemokines and their receptors (CXCR, CCR, CX_3C -- CX_3CR) [14]. SC migrating against chemokine (*e.g.* CXCL12 (SDF-1α) concentration gradient can accumulate in the focus of the glial tumor. This allows considering SC as a potential vehicle for delivery of a substance or signal to the focus of glioblastoma multiforme in systemic administration.

Here we studied antitumor activity of NPC and HSC *in vitro* and after implantation into the focus of experimental glioma C6.

MATERIALS AND METHODS

Experiments were performed using C6 rat glioma cells kindly provided by A. S. Khalanskii (Institute of Human Morphology, Russian Academy of Medical Sciences). $CD34^+$ cells were obtained at the Department of Cell Technologies and Regenerative Medicine, Institute of Fundamental and Applied Biomedical Studies, Russian State Medical University, Ministry of Health Care and Social Development of the Russian Federation.

Cell cultures. Rat glioma C6 cells were cultured in DMEM/F12 medium supplemented with 10% fetal bovine serum (FBS), 2 mM L-glutamine, 100 U/ml penicillin, and 100 μg/ml streptomycin at 37°C and 5% CO_2. In co-culturing experiments and for *in vivo* glioblastoma modeling, the cell monolayer was washed with Hanks saline to remove the serum and the cells were harvested with dissociating buffer TrypLEExpress (Invitrogen). The suspension was centrifuged at 100 rpm for 5 min. The supernatant was completely removed and the pellet was resuspended in the nutrient medium. For co-culturing with SC cells, a suspension of C6 cells in the growth medium DMEM/F12 with 10% FBS was used. For *in vivo* experiments, aliquots of cell suspension (4×10^5 cells in 1 ml serum-free DMEM /F12 serum with antibiotics) were prepared and stored at 4°C until stereotactic implantation into rat brain (3-4 h).

Human NPC and HSC. NPC were isolated from the olfactory epithelium of the superior nasal passage as described previously [1] and cultured in DMEM/F12 with 10% FBS and growth factors (Invitrogen) until the formation of cytospheres. Cytosphere cells were characterized by the expression of nestin, NF-200, β-tubulin, and GFAP according to the standard immunocytochemical protocol with secondary antibodies labeled with Alexa Fluor 488 and 633 (Invitrogen). Immunophenotyped NPC of cytospheres were dissociated in 0.25% trypsin-EDTA (Invitrogen) and cultured in serum-free medium with growth factors.

HSC were isolated from BM mononuclear fraction. Human BM was obtained from the iliac crest. The cell suspension was diluted 1:4 in Ca^{2+},Mg^{2+}-free medium and centrifuged in 50-ml tubes on Lymphoprep™ density gradient (d=1.077 g/ml, Axis-Shield) at 400*g* for 30 min at 20°C; mononuclear fraction cells were collected from the interphase, diluted with PBS, and washed twice by centrifugation for 10 min at 300*g* and 10°C. $CD34^+$-cells were isolated on columns in a magnetic field using MACS technology (Myltenyi Biotec).

Co-culturing of NPC and glioma cells. NPC (2.5×10^3, 1.25×10^3, and 0.6×10^3 cells in 100 ml) were seeded in wells of a 96-well plate (Costar), incubated for 1 h until cell attachment to the substrate, and then 5×10^3 glioma cells in the same volume of growth medium were added. Immortalized HEK293 cells not exhibiting signs of stem cells served as the control culture. In control wells, the equivalent number of glioma C6 cells was cultured under the same condition. The experiments were repeated 3 times. After 120-h co-culturing, MTT test was performed for evaluation of the number of viable cells in cultures.

MTT-test. The method is based on conversion of MTT reagent (3-(4,5-dimethylthiazol-2-yl)-2,5-diphenyltetrazolium bromide) into violet formazan crystals under the action of mitochondrial dehydrogenases in viable cells. Due to this, light absorption at 570 nm after incubation with MTT reagent is proportional to the number of stained functionally active cells. MTT was added for 4 h and then the cells were lysed routinely [10] and optical density (A_{570}) of the lysate was measured on a VictorX3 microplate reader (PerkinElmer).

Counting of S-phase cells using antibodies to BrdU. Bromodeoxyuridine (BrdU) incorporated into DNA during replication (S phase of mitosis) can be visualized using antibodies to BrdU–DNA complex. Adding BrdU to the incubation medium for a certain time interval we can determine proliferative activity of cells during this period by recording cells passing the S-phase after addition of the reagent to the medium.

After 120-h co-culturing of tumor and progenitor cells, BrdU was added to the growth medium at a final concentration of 50 μM and the cultures were incubated for 4 h at 37°C in a CO_2 incubator. Then,

the medium was removed and the cells were fixed with cold buffered fixative (70 ml ethanol and 30 ml glycine, pH 2.0) for 30 min at 20°C. Fixed cells were 3 times washed with PBS. For DNA denaturation, the cells were incubated in 2 M HCl at room temperature for 20 min, washed with PBS, and monoclonal antibodies to BrdU (Sigma) in PBS with 0.1% Tween-20 and 0.1% Triton X-100 were added in a concentration of 1 μ/ml. Cells incubated without BrdU and cells incubated with BrdU, but without antibodies to BrdU served as the control. After 1-h incubation, the cells were washed with the same buffer, incubated with second antibodies (goat anti-mouse Alexa 488, Invitrogen) for 1 h, washed with PBS, and fluorescent was recorded under a Leica DMI 6000 microscope. The cells were counted in 10 fields of view, the mean and standard deviation were calculated.

Glioblastoma modeling. Glioblastoma was modeled by intracerebral stereotactic implantation of C6 cells. The study was carried out on 30 female Wistar rats weighing 200 g at the beginning of the experiment. Suspension of glioma cells (2×10^5 cells per rat) was implanted into the striatum of ketamine-narcotized rats using a Narishige stereotactic apparatus according to Rat Brain Atlas by Swanson [12]: Ap -1; L 3.0; V 4.5, TBS-2.4 mm. The cells were injected in a volume of 5 μl with a microsyringe connected to infusomat at a rate of 3 μl/min.

Histochemical analysis. Histochemical analysis was performed on day 7 after glioma implantation and at the end of the experiment (day 14). The rats under deep narcosis were perfused through the aorta with 4% paraformaldehyde. Serial brain sections (20 and 40 μ) were prepared on a Microm HM560 cryostat microtome. For morphological analysis, the sections were stained after Nissl (0.1% cresyl violet on 0.1 M acetate buffer, pH 3.3) and with 0.1% toluidine blue on the same buffer.

Implantation of SC into glioma. The rats with experimental glioma were randomly divided into 3 groups (10 rats per group). Group 1 rats received no treatment. Group 2 rats received HSC (n=5) and NPC (n=5). Immediately before implantation into the glioma, HSC and NPC were labeled with vital fluorescent tracers CFDA SE (Invitrogen) and Dil (Sigma) in concentrations of 5 and 1 μM, respectively, according to manufacturers' instructions. The cells were injected into the peritumoral space on day 7 after glioma implantation according to the following coordinates: Ap -1; L 3.0; V 3.8-3.3, TBS -2.4 mm with automatic injector at a rate of 0.5 μl/min. Preliminary experiments showed that these depth coordinates at the specified term of glioma allow introduction of SC into the tumor edge and peritumoral space directly above the glioma A total of 5×10^5 cells were implanted to each animal. An additional reference group comprised rats receiving injections of HPC and HSC (5 animals for each cell type) treated with ribosome-inactivating protein ricin in a concentration of 5 mg/ml for 10 min. This protein consists of 2 subunits, binding (B) and catalytic (A). The binding subunit, lectin, is responsible for interaction of the toxin with plasma membrane receptors, its internalization, intracellular transport, and the release from the luminal surface of cell organelles to ribosoma [8,9]. One A-subunit can inactivate up to 1500 ribosomes per minute, which leads to apoptosis activation and cell death. SC treated with ricin according to the above protocol retain viability for at least 16 h and die via apoptosis in 24 h. Cell death is accompanied by membrane disintegration and release of apoptosis inductor into incroenvironment, which, in turn, causes death of adjacent cells.

Visualization of implanted HSC and HPC was performed in 7 days after implantation on cryostat brain sections with 14-day glioma under a Leica DMI 6000 fluorescent microscope, Dil-positive NPC and CFDA-positive HSC were visualized using N2.1 and GFP filters, respectively.

Morphometry. Glioma volume was determined on 20-μ serial section of rat brain stained after Nissl. Since the tumor formed after implantation of glioma cells into the striatum always had ellipsoid shape, its volume (V) was calculated by formula **(1)**:

$$V=4/3\pi abc \qquad \textbf{(1)},$$

where a, b, and c are ellipsoid semiaxes.

For calculation of glioma volume, the section with maximum glioma area was chosen and the greater (a) and lesser (b) semiaxes of the ellipsoid were measured. Then, the sagittal semiaxis was determined by summation of the thickness of frontal sections from the anterior to the posterior pole (c). Parameters a, b, and c (in mm) were substituted in formula **(1)** and glioma volume was calculated (in mm^3). The accuracy of calculation using the formula for ellipsoid volume was ≥95%, which was proven by comparison of the true glioma area and area calculated using the formula for ellipse area.

RESULTS

Co-culturing of NPC and glioma cells. The results of MTT tests after 120-h incubation demonstrated considerable decrease in optical density in wells containing glioma C6 cells and NPC (Fig. 1, *3*). In wells containing 5×10^3 MPC and 2.5×10^3 glioma cells (*i.e.* 1:2 ratio), the content of viable cells after 120-h incubation decreased by 25% in comparison with both the control (C6 glioma cells without NPC Fig. 1, *1*)

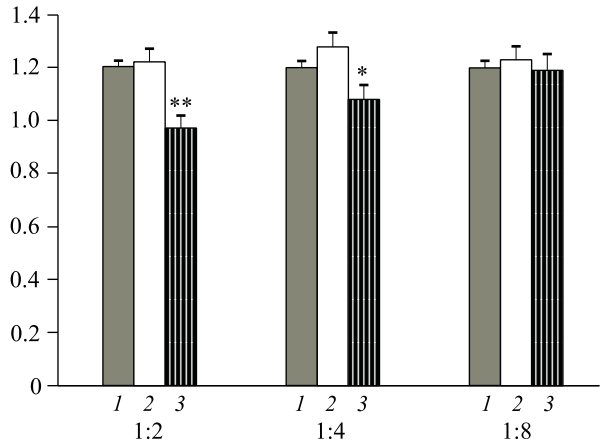

Fig. 1. MTT-analysis of cell viability after co-culturing of glioma C6 cells with NPC and HSC in different proportions. Abscissa: progenitor to tumor cell ratio; ordinate: optical density. *1*) C6; *2*) C6+HEK293; *3*) C6+NPC. **p*<0.05, ***p*<0.01 compared to the control (C6).

and C6 glioma cells cultured with HEK293 cells (Fig. 1, *2*). In some independent experimental series, these differences were significant ($p<0.01$).

Significant differences from control wells were also observed after co-culturing of C6 glioma cells with NPC at a ratio of 1:4, but in this case the count of viable glioma cells was higher than after C6 co-culturing with NPC at a ratio of 1:2. After 120-h co-culturing of C6 with NPC at a ratio of 1:8, no significant differences from the control in the number of viable cells were found.

In control wells containing C6 glioma cells and HEK293 cells, no dose-dependent effect was found and optical density in each measurement was somewhat higher than in the control (C6 cells without co-culturing, Fig. 1).

Analysis of mitotic activity with BrdU suggests that SC are characterized by low proliferation rate (no more that 1% cells passed S-phase of mitosis during 4-h incubation with BrdU), especially in comparison with aggressive C6 glioma cells (~30% dividing cells over 4 h at the same initial concentration); therefore, the contribution of NPC into overall mitotic activity of co-cultured cells can be neglected.

Analysis of proliferative activity of glioma cells co-cultured with NPC showed that the rate of tumor cell proliferation after 120-h co-culturing was significantly lower than in control wells (Fig. 2). We observed a decrease in both the absolute number of cells stained with DAPI, and the absolute number of cells incorporating BrdU. These changes were absent in case of glioma C6 co-culturing with embryonic kidney epithelial HEK293 cells: the total number of DAPI-stained cells and the number of BrdU-positive cells did not differ from the control glioma C6 monoculture.

Analysis of the relative proliferation rate, *i.e.* the number of cells passing DNA replication phase over the observation period from the total number of cells, yielded interesting results: 16.3±1.4% for glioma C6 and NPC co-culture *vs.* 28.2±1.8% for C6 monoculture and 20.5±2.2% for C6 and Hek293 co-culture. Thus, the relative number of dividing cells from the total number of glioma cells decreased by 1.7 times after co-culturing with NPC. This suggests that co-culturing of glioma C6 with NPC and HSC leads to a considerably decrease in proliferative activity of tumor cells.

Implantation of NPC into experimental glioma focus. HSC were isolated by immunomagnetic sorting with immobilized antibodies to CD34 immediately before implantation. Control flow cytofluorometry showed that CD34-positive cells constituted 95.4± 1.0% cells.

NPC were obtained from the cell bank and cultured in media containing a growth factor cocktail (Invitrogen). Immunotyping of these cells with antibodies to neurofilaments-200, β-tubulin, nestin, and GFAP allowed us to refer these cells as neural and astroglial lineage progenitor cells (Fig. 3); it should be noted that many cells simultaneously expressed

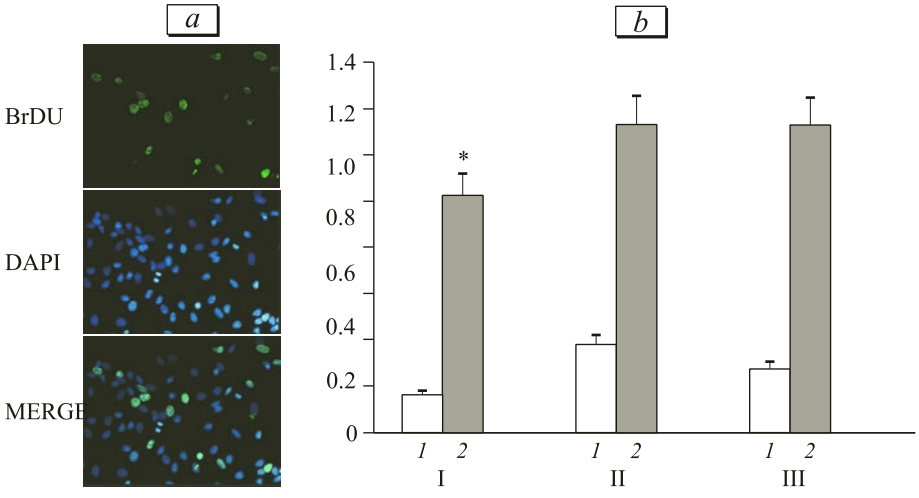

Fig. 2. Proliferative activity of glioma C6 cells after co-culturing with NPC. *a*) visualization of cells containing BrdU after co-culturing of C6 with NPC. BrdU is visualized with primary MAb (Sigma) and second antimouse Ab with Alexa Fluor 488 (Invitrogen). Cell nuclei are stained with DAPI (Invitrogen; ×400); *b*) mean number of glioma cells in field of view after co-culturing with NPC (C6+NPC; I), in monoculture (C6; II), and after co-culturing with HEK293 (C6+HEK293; III). *1*) BrdU, *2*) DAPI. **p*<0.05.

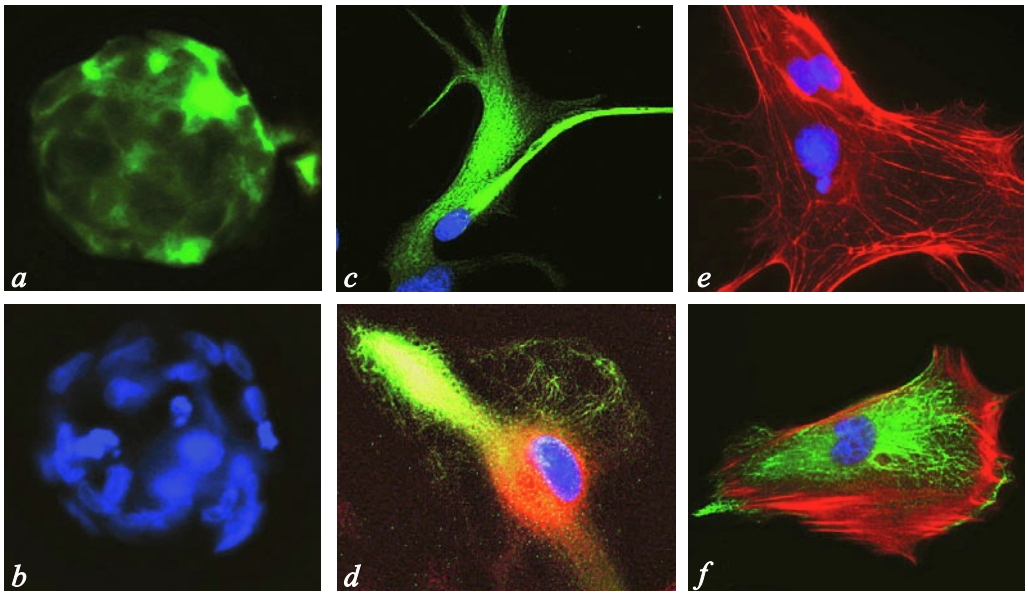

Fig. 3. Immunophenotyping of NPC from human olfactory epithelium. *a*) NF-200-positive neurosphere formed after the 3rd passage of NPC (neurofilaments, 200 kDa); *b*) cell nuclei of the sphere post-stained with DAPI; *c*) nestin-positive NPC (Alexa 488); *d*) GFAP-positive NPC (Alexa 488); *e*) NPC simultaneously expressing genes of two intermediate filament proteins (Nistin, Alexa 488+GFAP, Alexa 594); *e*) β-tubulin (Alexa 488) and actin (Phalloidin TRITC).

both assayed intermediate filament proteins: GFAP and nestin (Fig. 3, *d*).

Immunophenotyped HSC and NPC were implanted into the focus of 7-day glioma and after 1 week. On day 14 after implantation of glioma cells, the animals were perfused, serial sections of the brain were performed, and morphometry of glioma volume was carried out.

On day 7 at the moment of SC implantation, glioma volume was 50±7 mm^3 (Fig. 4, *a*). Thus, glioma volume increased 10-fold over 7 days after implantation (the volume of injected suspension was 5 μl). If the number of glioma cells in 7-day tumor increased proportionally to its volume and attained 2×10^6 cells, the SC-tumor cell ratio after implantation of 5×10^5 SC per rat was 1:4.

On day 14 after glioma implantation in the control group (without SC injection), the volume of glioma was 220.3±29.7 mm^3 (Fig. 4, *b*). In rats receiving NPC and HSC, the volume of glioma at this term was 170.4±21.4 and 165.3±19.7 mm^3, respectively (Fig. 4, *c*). These values were significantly below the corresponding parameters in the control group ($p<0.05$).

In animals receiving ricin-treated SC, glioma volume significantly increased (298.6±34.5 and 316.6±30.2 mm^3 after implantation of NPC and HSC, respectively, $p<0.05$ in comparison with the control and experimental groups; Fig. 4, *e*)

SC labeled with CFDA SE and Dil were visualized on frozen brain sections under a DMI 6000 fluorescent microscope (Leica Microsystems) and LSM Pascal

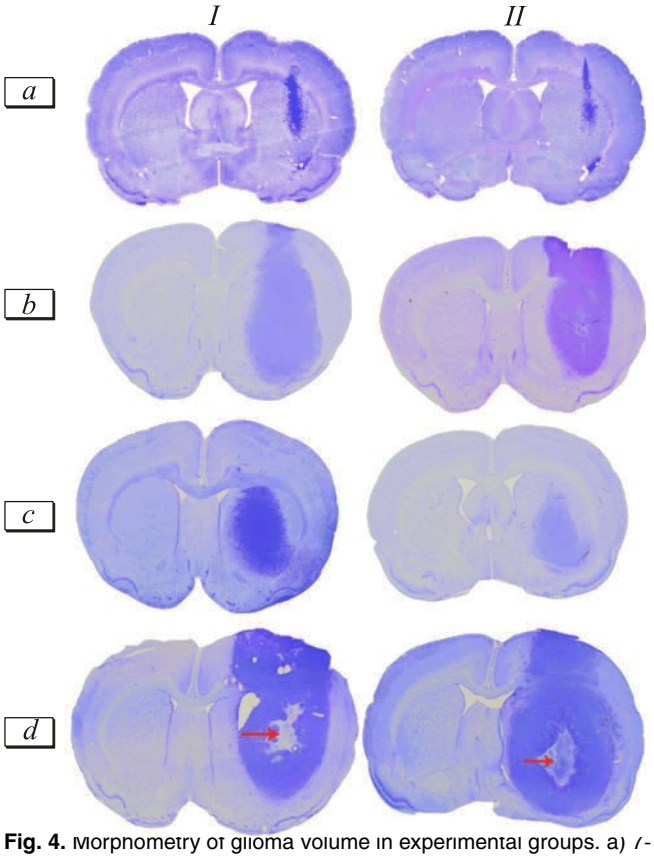

Fig. 4. Morphometry of glioma volume in experimental groups. a) 7-day glioma C6 (term of NPC and HSC implantation); *b*) experimental glioma in the control without cell implantation; *c*) experimental glioma after implantation of NPC (*I*) and HSC (*II*): $p<0.05$ in comparison with the control group; *d*) glioma after implantation of NPC (*I*) and HSC (*II*) pretreated with apoptosis inductor ricin (5 mg/ml). Arrows show nidus necrose. Necrotic foci are shown by arrows.

scanning laser confocal microscope (Karl Zeiss). In experimental groups receiving fluorolabeled NPC and HSC, these cells were detected in brain sections in 100% cases (Fig. 5, Fig. 6).

Hemopoietic CD34$^+$ SC were detected in the site of injection and along the periphery of 14-day glioma, which attested to migration of these cells in the peritumoral zone during glioma growth (Fig. 5). These

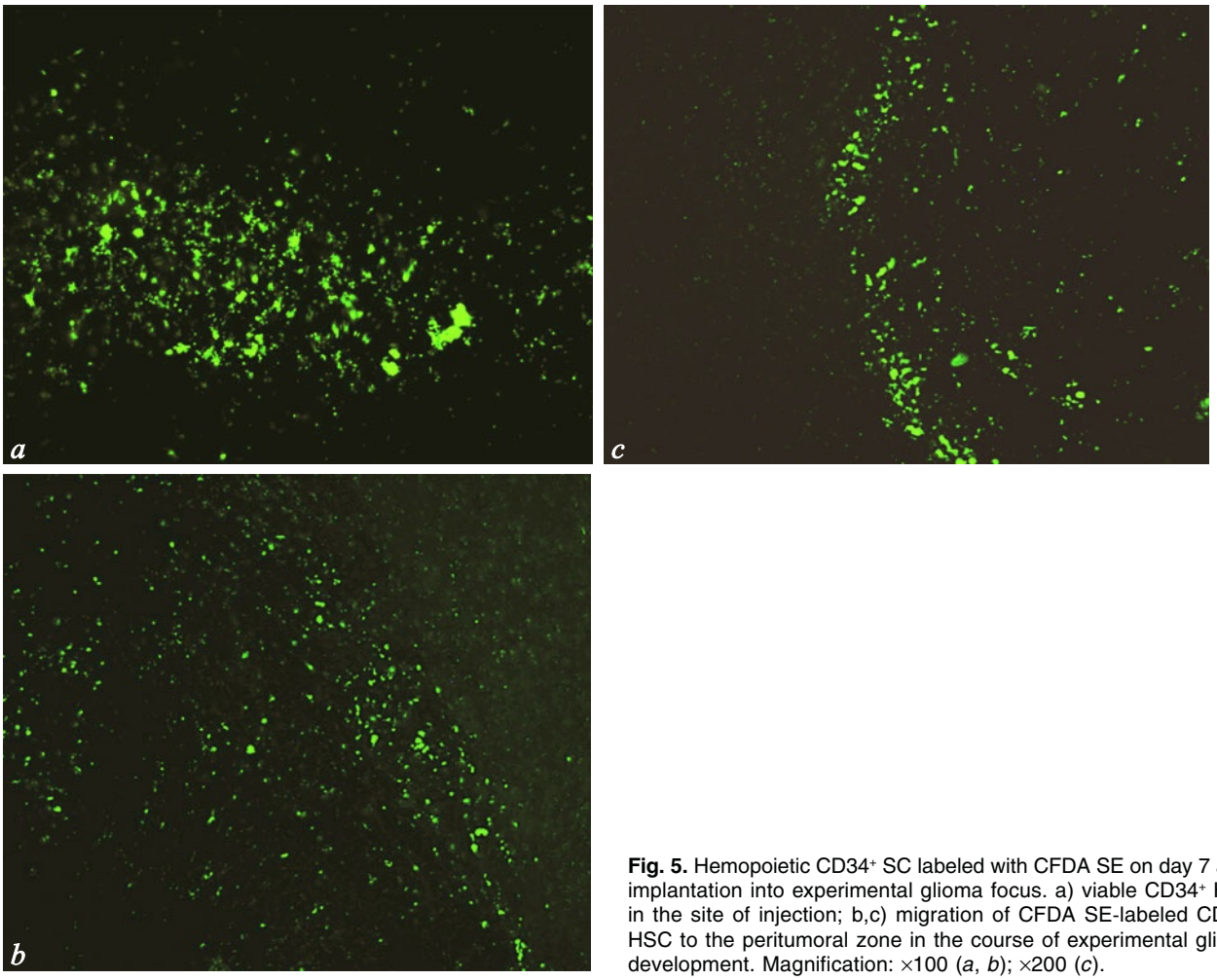

Fig. 5. Hemopoietic CD34$^+$ SC labeled with CFDA SE on day 7 after implantation into experimental glioma focus. a) viable CD34$^+$ HSC in the site of injection; b,c) migration of CFDA SE-labeled CD34$^+$ HSC to the peritumoral zone in the course of experimental glioma development. Magnification: ×100 (*a*, *b*); ×200 (*c*).

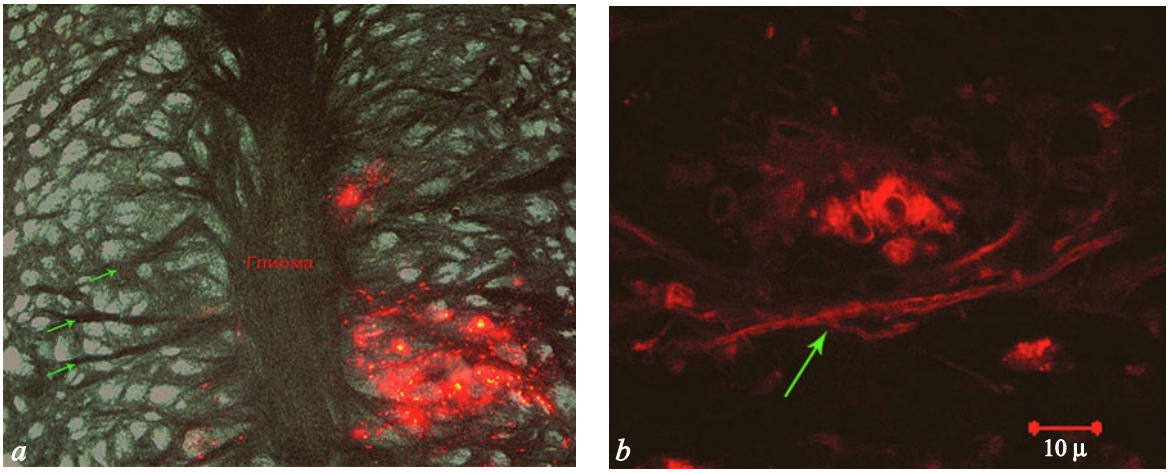

Fig. 6. Visualization of DiI-labeled NPC in the peritumoral space on day 7 after implantation. *a*) peritumoral localization of DiI-labeled NPC: arrows show sites of invasion of glioma cells. NPC are distributed along the areas of invasion (superposition of phase-contrast and fluorescent microscopy, ×100); *b*) scanning laser confocal microscopy: arrow shows processes of DiI-positive differentiated NPC, ×630.

cells had round shape and did not form processes, but it can certainly be concluded that they retained viability, because CFDA SE fluorescence can be detected in only viable cells.

Dil-labeled NPC were also seen along the glioma periphery. In contrast to HSC, NPC were also found in sites of perivasal invasion of glioma cells, wich attested to their migration together with glioma cells (Fig. 6, *a*).

Scanning laser confocal microscopy of Dil-labeled NPC showed that some of these cells form long processes in the peritumoral space. This suggests that these cells enter differentiation and are presumably transformed into reactive astrocytes forming the peritumoral glial bank (Fig. 6, *b*).

These findings drove us to a conclusion that NPC and HSC implanted into glioma and peritumoral space survive for at least 1 week after implantation, migrate with glioma cells, and accumulate in the peritumoral space. NPC migrate in perivasal spaces and undergo partial differentiation with the formation of long processes.

Implantation of cytostatic-pretreated cells was used as a model system for targeted SC-mediated delivery of cytostatic antibiotics and killer genes (expression of these genes kills both the vehicle cells and adjacent tumor cells. These results suggest that this approach will probably not produce considerable therapeutic effect, because using cytotoxic drugs we cannot exclude certain selection promoting survival of the most aggressive and apoptosis-resistant glioma cells.

We can conclude that implantation of NPC and HSC leads to considerable inhibition of experimental glioma C6 in comparison with the control. The mechanisms of tumor-suppressive effect of NPC and HSC require further investigation.

The study was partially supported by NeuroVita Clinics of Restorative and Interventional Neurology and Therapy.

Authors are grateful to Dr. M. M. Moisenovich (Biological Faculty, M. V. Lomonosov Moscow State University) for his help in experiments with ricin.

REFERENCES

1. I. V. Viktorov, E. A. Savchenko, O. V. Ukhova, *et al., Klet. Tekhnol. Biol. Med*., No. 4, 185-193 (2006).
2. M. C. Chamberlain, *Neurosci. Focus*., **20**, No. 4, E19 (2006).
3. S. R. Chirasani, A. Sternjak, P. Wend, *et al., Brain*, **133**, Pt. 7, 1961-1972 (2010).
4. P. B. Dirks, *Mol. Oncol.*, **4**, No. 5, 420-430 (2010).
5. U. Galderisi, M. Cipollaro, and A. Giordano, *Cell. Death Differ.,* **13**, No. 1, 5-11 (2006).
6. *Joo-Hee Walzlein, Endogenous neural precursor cells suppress glioblastoma. (PhD in Medical Neurosciences).* Berlin (2007).
7. S. Li, Y. Gao, T. Tokuyama, *et al., Cancer Lett*., **251**, No. 2, 220-227 (2007).
8. M. Moisenovic, A. Tonevitsky, I. Agapov, *et al., Eur. J. Cell. Biol.,* **81**, No. 10, 529-538 (2002).
9. M. Moisenovic, A. Tonevitsky, N. Maljuchenko, *et al., J. Histochem. Cell Biol.,* **121**, No. 6, 429-439 (2004).
10. T. Mosmann*, J. Immunol. Methods*, **65**, Nos. 1-2, 55-63 (1983).
11. I. Singec, R. Jandial, A. Crain, *et al., Annu. Rev. Med*., **58**, 313-328 (2007).
12. L. W. Swanson, *Brain Maps: Structure of the Rat Brain*. 2nd Ed. Amsterdam (1998).
13. G. Xu, X. D. Jiang, Y. Xu, *et al., Cell Biol. Int.*, **33**, No. 4, 466-474 (2009).
14. S. Yip, R. Sabetrasekh, R. L. Sidman, and E. Y. Snyder, *Eur. J. Cancer*, **42**, No. 9, 1298-1308 (2006).